

Effect of nuclear dissipation on neutron emission prior to fission

P. Grangé and S. Hassani

Centre de Recherches Nucléaires et Université Louis Pasteur, Strasbourg, France

H. A. Weidenmüller

Max-Planck-Institut für Kernphysik, Heidelberg, Federal Republic of Germany

A. Gavron, J. R. Nix, and A. J. Sierk

Los Alamos National Laboratory, Los Alamos, New Mexico 87545

(Received 7 February 1986)

We present a formalism for calculating three effects of nuclear dissipation on neutron emission prior to fission: (1) Kramers's modification of the Bohr-Wheeler statistical-model result for the fission width; (2) the transient time required to build up the quasistationary probability flow over the barrier; and (3) the mean time required for the system to descend from the saddle point to scission. Each of these effects increases the average multiplicity of neutrons emitted prior to fission relative to that calculated with a standard statistical model. The multiplicity calculation includes the dependence of the ratio a_f/a_n of level-density parameters for fission and neutron emission upon dissipation that is imposed by the low-energy fission probability. We use this formalism to analyze recent experimental results of Gavron *et al.* for the reaction $^{16}\text{O} + ^{142}\text{Nd} \rightarrow ^{158}\text{Er}$ at 207 MeV, where 2.7 ± 0.4 neutrons are emitted prior to fission compared to 1.6 neutrons calculated with a standard statistical model. This determines the limit $\beta \lesssim 5 \times 10^{21} \text{ s}^{-1}$ for the reduced nuclear dissipation coefficient β defined as the ratio of the dissipation coefficient to the inertia.

I. INTRODUCTION

Nuclear physicists have been struggling for years to determine the magnitude of nuclear dissipation in large-amplitude collective motion—to learn whether in fission and heavy-ion reactions nuclei are underdamped like water or overdamped like honey. Despite numerous experimental clues, the answer has thus far proved elusive because of the difficulty of distinguishing dissipative effects from analogous effects caused by collective degrees of freedom.

We have developed a new approach to this question in terms of a formalism that determines the magnitude of nuclear dissipation from the average number of neutrons emitted prior to fission. These neutrons are affected by dissipation in three significant ways. First, as shown by Kramers,¹ dissipation increases the fission lifetime relative to that calculated with the standard Bohr-Wheeler statistical model,² which arises because fission is a quasistationary diffusion process over the barrier. Second, additional time is available for neutron emission during the transient time needed for the system to build up the quasistationary probability flow over the barrier, which is affected by dissipation.^{3–6} Third, still more neutrons can be emitted during the time required for the system to descend from the saddle point to scission, which is increased by dissipation.^{7–9}

In several experiments at high excitation energies,^{10–14} significant enhancements have been detected in the number of neutrons emitted prior to fission relative to the number calculated with a standard statistical model. Previous suggestions for these enhancements have included

neutron emission both during the descent from saddle to scission^{10,11} and during the acceleration of the fission fragments.¹³

In the most recent of these experiments,¹⁴ the energies and angular distributions of the neutrons emitted in coincidence with fission fragments and evaporation residues were measured for four reactions and were analyzed to yield the number of neutrons emitted prior to fission and the number of neutrons emitted from the fission fragments. We have selected for detailed analysis the reaction $^{16}\text{O} + ^{142}\text{Nd} \rightarrow ^{158}\text{Er}$ at 207 MeV, where 2.7 ± 0.4 neutrons are emitted prior to fission compared to 1.6 neutrons calculated with a standard statistical model. Since this reaction has the highest excitation energy and highest enhancement in the number of neutrons emitted prior to fission, its analysis permits us to determine an upper limit of nuclear dissipation with greater precision than for the other reactions that were considered.

We present in Sec. II a general discussion of three effects of nuclear dissipation on neutron emission prior to fission. This is followed in Sec. III by a calculation of the average neutron multiplicity prior to fission, as well as a comparison with experiment. Our conclusions are presented in Sec. IV.

II. THREE PHYSICAL EFFECTS

A. Kramers's modification of the Bohr-Wheeler statistical-model result

Bohr and Wheeler based their derivation of the fission width Γ_f on phase-space arguments.² Kramers was the

first author to recognize that the value of Γ_f is influenced by nuclear dissipation.¹ We denote by β the nuclear dissipation coefficient divided by the inertia and refer to β as the reduced dissipation coefficient; it has the unit of inverse time.

Describing nuclear fission as a diffusion process over the fission barrier and using the quasistationary solution of the Fokker-Planck equation, Kramers showed that the dependence of Γ_f on β is given by

$$\Gamma_f = \Gamma_f^0 \left(\left\{ 1 + [\beta/(2\omega_0)]^2 \right\}^{1/2} - \beta/(2\omega_0) \right), \quad (1)$$

where ω_0 is the frequency of the inverse harmonic-oscillator potential that osculates the fission barrier at the saddle point. Equation (1) is valid for all but very small values of $\beta/(2\omega_0)$; in the limit $\beta \rightarrow 0$, the width Γ_f should approach 0 instead of Γ_f^0 . Since we are not concerned here with such small values of β , we use Eq. (1) without further qualification. In Kramers's derivation, the constant Γ_f^0 differs slightly from the expression derived by Bohr and Wheeler. In the present paper, we identify Γ_f^0 with the Bohr-Wheeler expression.

The dependence of Γ_f on $\beta/(2\omega_0)$ is displayed in Fig. 1. For the value $\beta/(2\omega_0) = 1$, which corresponds to critical damping in the inverted oscillator turned upright, the reduction in the fission width is by over a factor of 2. Since it is difficult to determine reliably either the temperature dependence of the fission barrier or the nuclear level density at the saddle point, both of which sensitively influence the value of Γ_f^0 , it has not been possible to measure this reduction factor and thereby β .

B. Transient time required to build up the quasistationary probability flow

The study of transients in the fission process offers the hope of overcoming this difficulty and of deducing a value of β from measured neutron multiplicities prior to fission. This would be of considerable interest since data on β are presently available only for heavy-ion collisions, for which the overlap of the colliding nuclei is small and the velocity of relative motion is high, and from the analysis of the fission process during the descent from saddle to scission. In contradistinction, an analysis of

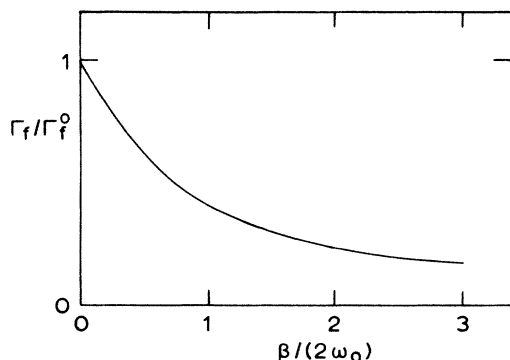


FIG. 1. Dependence of the fission width Γ_f upon the reduced dissipation coefficient β , calculated from Eq. (1).

neutron multiplicities should yield more information on the value of β deep in the nuclear interior.

This hope is based on the following idea.^{3,4} Following Kramers's idea, we describe the fission process in terms of a diffusive probability current over the fission barrier, which is calculated by solving a Fokker-Planck equation. At time $t=0$, defined by the onset of a nuclear reaction inducing fission, the fission degree of freedom is in its ground state and thus located near the minimum of the fission potential. If the nucleonic degrees of freedom that are excited by the reaction equilibrate quickly in comparison with the characteristic time scales of the fission process, we may view the fission degree of freedom as being in contact with a heat bath of temperature $T = (E^*/a)^{1/2}$, where E^* is the nuclear excitation energy and a is the level-density parameter. The strength of the coupling is determined by β .

The solution of the Fokker-Planck equation describes the gradual spreading of the original probability distribution, with the probability current over the barrier rising smoothly from 0 at time $t=0$ to the quasistationary value calculated by Kramers. We denote by τ the time required for the current to reach 90% of its quasistationary value, and refer to τ as the transient time. The quantity τ shows a characteristic dependence on $\beta/(2\omega_1)$, where ω_1 is the frequency of the harmonic-oscillator potential that osculates the fission potential at its ground-state minimum.^{4,5} For $\beta/(2\omega_1) \lesssim 1$, corresponding to underdamped classical motion near the minimum, τ is inversely proportional to $\beta/(2\omega_1)$. For $\beta/(2\omega_1) \gg 1$, the transient time τ increases linearly with $\beta/(2\omega_1)$. This is a consequence of the overdamping of the motion, since the probability current becomes more and more viscous with increasing β .

During the time interval τ needed for the probability current over the fission barrier to attain its quasistationary value, neutron emission is possible. If τ is comparable to the average lifetime $\tau_n = \hbar/\Gamma_n$ for neutron emission, where Γ_n is the neutron width, we expect to find of the order of one more neutron emitted prior to fission than is calculated with a statistical model. In this way, a measurement of the neutron multiplicity prior to fission may yield information on τ and thereby on β .

Whereas the transient time τ depends very smoothly on the excitation energy E^* , the neutron width Γ_n rises steeply with E^* . According to Ref. 4, τ_n becomes comparable to τ for reasonable values of β at excitation energies around 50 MeV for $A=226$. It is for such and higher energies that a measurement of neutron multiplicities is promising in the present context. Similar conclusions are drawn in Refs. 15 and 16.

Our above assumption that fission and neutron evaporation start from a prescribed equilibrium distribution centered at the rotating ground-state minimum is valid only when the equilibrium time τ_{eq} is short compared to both the neutron-emission time τ_n and the transient time τ . Although these conditions are often satisfied for light-particle-induced fission, they could be much less well satisfied for the heavy-ion-induced reaction $^{16}\text{O} + ^{142}\text{Nd} \rightarrow ^{158}\text{Er}$ at 207 MeV considered here. In particular, neutrons could be emitted during the time required for the system to evolve from the initial configuration of two

touching spheres to the rotating ground state minimum. Furthermore, especially for the higher partial waves, where the potential pocket at the rotating ground state almost disappears, the system may never even reach this shape but instead may fission immediately. Because of the diffusive reaction dynamics, a given partial wave may sometimes lead to a compound nucleus, while at other times may lead directly to fission. It is therefore not possible to rigorously associate a certain type of reaction mechanism with a given partial wave.

The above issues could be addressed by solving a multidimensional Fokker-Planck equation for the time evolution of the distribution function in phase space of collective coordinates and momenta, starting from an initial configuration of two touching spheres. For this purpose, the techniques used recently to solve a two-dimensional Fokker-Planck equation¹⁷ could perhaps be successfully generalized. Such an approach represents an outstanding problem for the future and will probably be required to systematically reproduce the experimental results for all the fissioning systems that have been considered.¹⁰⁻¹⁴ We hope that the results from the present analysis based on a number of idealizations will stimulate the execution of this ambitious program.

For our present reaction and the approximations made here, the primary contributions to fission come from angular momenta lying in the range $65\hbar \lesssim J \lesssim 76\hbar$, with the exact values depending on the viscosity coefficient and transient time. For three angular momenta in this range, we show in Fig. 2 fission barriers calculated with a macroscopic model that includes repulsive Coulomb and centrifugal energies and an attractive Yukawa-plus-exponential potential.¹⁸ With the zero of potential energy taken as the energy of the nonrotating spherical nucleus, the barriers are plotted as functions of a fission coordinate r defined as the distance between the centers of mass of the two halves of the dividing nucleus. The nuclear shapes are specified by means of an axially asymmetric generalization of the parameterization of Trentalange *et al.*,¹⁹ where the square of the perpendicular distance from the symmetry axis z to the nuclear surface is expanded in a series of even Legendre polynomials $P_{2n}(z/z_0)$, with z_0 equal to one-half the distance between the two ends of the shape. The shapes between the ground state and the saddle point for a given angular momentum are taken to be the equilibrium configurations for larger values of angular momentum. The shapes beyond the saddle points are generated by following the dynamical evolution of nondissipative ¹⁵⁸Er nuclei constrained to remain axially symmetric about an axis that is rotating in space.^{20,21} The ter-

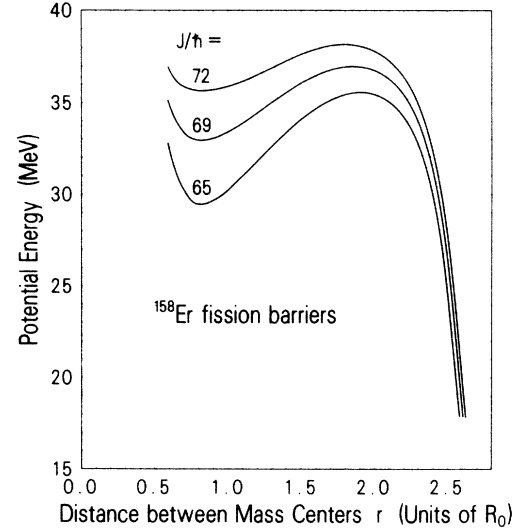


FIG. 2. Fission barriers for ¹⁵⁸Er corresponding to three values of angular momentum J . The quantity $R_0 = 1.16$ fm $(158)^{1/3} = 6.27$ fm.

minations of the fission barriers in the lower right-hand corner of Fig. 2 correspond to scission configurations with zero neck radius.

The resulting values of the fission-barrier height E_f are shown in the second column of Table I. The third column gives the values of the barrier frequency ω_0 that were used in the calculation of the transient time τ . These were obtained by performing normal-coordinate transformations at saddle-point shapes constrained to axial symmetry, with nuclear inertias calculated for nearly irrotational flow by means of the Werner-Wheeler approximation.²² For the calculation of the mean saddle-to-scission time $\bar{\tau}$ to be discussed in subsection C, it is more appropriate to use values of the barrier frequency ω_0 that reproduce for parabolic barriers with constant inertia the actual saddle-to-scission times for nondissipative descents calculated by numerically solving the classical dynamical equations of motion for a unified macroscopic model.^{20,21} The corresponding values obtained in this way are shown in the fourth column of Table I. The fifth column gives the values of the ground-state frequency ω_1 that were used in the calculation of the transient time τ . These were obtained by approximating the barriers by portions of inverted and upright parabolas that join smoothly, with constant nuclear inertias.⁸

In the subsequent calculations of the transient time τ

TABLE I. Parameters characterizing the ¹⁵⁸Er fission barriers and inertias, used for the calculation of the transient time τ and the mean saddle-to-scission time $\bar{\tau}$.

Angular momentum J (\hbar)	Barrier height E_f (MeV)	Barrier frequency ω_0 for transient calculation (10^{21} s ⁻¹)	Barrier frequency ω_0 for saddle-to-scission calculation (10^{21} s ⁻¹)	Ground-state frequency ω_1 (10^{21} s ⁻¹)
65	6.10	1.15	1.82	0.88
69	4.05	1.03	1.67	0.75
72	2.51	0.91	1.54	0.61

and the mean saddle-to-scission time $\bar{\tau}$, both the nuclear inertia and the dissipation are assumed to be independent of deformation. Because of this, we are able to address directly only the magnitude of nuclear dissipation and not its mechanism. The latter must then be inferred indirectly by relating the magnitude deduced here to the magnitude corresponding to a given dissipation mechanism, suitably averaged over deformation.

To enable the reader to form an idea of the competition between the transition time τ and the average lifetime for the emission of the first neutron, we present in Fig. 3 our calculated dependence of the transient time τ upon the reduced dissipation coefficient β for angular momentum $J=65\hbar$. We see that for small values of β the transient time has the nearly hyperbolic behavior referred to above, although the underdamping of the motion for this range of β gives rise to slight oscillations. This is followed by a fairly flat plateau, which eventually turns into a linear increase as β is increased further. We also note that τ is larger than the lifetime τ_n for the emission of the first neutron. This strongly suggests that transients will increase the theoretical multiplicity of neutrons prior to fission as compared to the result calculated with a statistical model.

In order to quantify the influence of the time delay τ in the fission process on the neutron multiplicity, two steps must be taken. First, it is necessary to have available an analytical form for the time dependence of the fission rate. Second, the time-dependent cascade-type coupled equations for multiple neutron emission must be solved using the analytical form for the fission rate obtained in the first step. We break up the problem in this way since the direct approach to the desired answer—a simultaneous numerical solution of the Fokker-Planck equation for fission and the coupled equations for neutron emission—is computationally difficult, despite recent progress in this

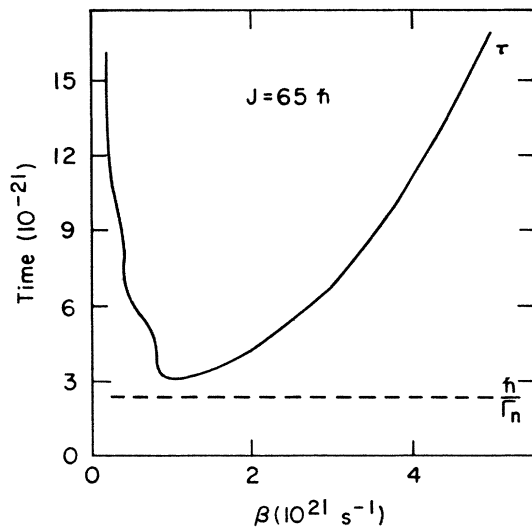


FIG. 3. Dependence of the transient time τ upon the reduced dissipation coefficient β , for angular momentum $J=65\hbar$. The constant dashed curve gives the corresponding lifetime τ_n for the emission of the first neutron; this lifetime increases substantially for the emission of subsequent neutrons.

direction.²³ In the remainder of this subsection, we describe the parametrization of the fission rate that we have used. The coupled equations for neutron emission are introduced in Sec. III.

Let $f(x, v; t)$ denote the normalized time-dependent solution of the Fokker-Planck equation, with x the position and v the velocity of the fission degree of freedom. The quantity

$$\Pi(x_0; t) = \int_{-\infty}^{x_0} dx \int_{-\infty}^{\infty} dv f(x, v; t)$$

gives the probability for finding the system to the left of the saddle point x_0 . The time-dependent fission rate, evaluated at the saddle point, is then

$$\lambda_f(t) = -\frac{d}{dt} \ln[\Pi(x_0; t)]. \quad (2)$$

The rate $\lambda_f(t)$ vanishes at time $t=0$, whereas for large t it attains the quasistationary value Γ_f/\hbar derived by Kramers, with Γ_f given by Eq. (1).

In Ref. 4, a parametrization for $\lambda_f(t)$ was obtained from analytical arguments. This parametrization was found to be in reasonable agreement with numerical solutions of the Fokker-Planck equation generated in the same paper, at least as long as the classical motion near the ground state is not overdamped, corresponding to $\beta \lesssim 2\omega_1$. In recent work by Bhatt, Grangé, and Hiller,²⁴ this parametrization was extended to the overdamped case. We use a similar parametrization in the present paper, but with a slight modification required by the condition that for $t \rightarrow \infty$, the width $\lambda_f(t)$ should approach the constant Γ_f defined in Eq. (1).

Let $\lambda_f^{\text{BGH}}(t)$ denote the quantity defined by the right-hand side of Eq. (3.17) of Ref. 24 for the underdamped case and of Eq. (3.26) of Ref. 24 for the overdamped case. Since for large t the rate $\lambda_f^{\text{BGH}}(t)$ does not approach the value Γ_f/\hbar , we instead use here the rate

$$\lambda_f(t) = \lambda_f^{\text{BGH}}(t) (\Gamma_f^{(0)}/\hbar) (2\pi/\omega_1) \exp(E_f/T), \quad (3)$$

which fulfills the conditions just mentioned. Here E_f is the height of the fission barrier and T is the nuclear temperature measured in energy units.

The rate $\lambda_f^{\text{BGH}}(t)$ depends on the initial distribution $f(x, v; 0)$, on the values of the four quantities ω_0 , ω_1 , E_f , and T , and on the reduced mass μ of the system in the fission degree of freedom. The variances and correlation functions present in Eqs. (3.17) and (3.26) of Ref. 24 are taken simply as those of a harmonic oscillator of frequency ω_1 . For the temperature and barrier height envisaged here this is a reasonably good approximation to the more elaborate scheme proposed in Ref. 24. For $f(x, v; 0)$ we use a Gaussian distribution centered at the minimum of the fission barrier, with a width corresponding to an equilibrium distribution at temperature $T=0.3$ MeV. This distribution is supposed to mimic the distribution in position and velocity variables in the nuclear ground state. For μ we use the reduced mass corresponding to symmetric fission of the appropriate nucleus along the decay chain.

To calculate the nuclear temperature T , we determine the internal excitation energy E^* by subtracting from the

total nuclear excitation energy the energy of the rotating ground-state minimum, which is shown in Fig. 2 for three values of angular momentum. For the level-density parameter a , we use two different values, corresponding to neutron emission and fission. When calculating neutron widths, as will be described in Sec. III, we use $a_n = 158/(7.5 \text{ MeV})$. When calculating the temperature in the Bohr-Wheeler formula and in $\lambda_f(t)$, we use slightly larger values of a_f for reasons that will be described later. As discussed earlier, values of the frequencies ω_0 and ω_1 that enter our calculation are listed in Table I, together with values of the barrier height E_f corresponding to the first step of the chain.

For a typical example corresponding to angular momentum $J = 65\hbar$ and reduced dissipation coefficient $\beta = 0.5 \times 10^{21} \text{ s}^{-1}$, we show the behavior of $\lambda_f(t)$ obtained in this way in Fig. 4, where we plot the width $\hbar\lambda_f(t)$ vs time. The steep rise of the curve is superposed by slight wiggles which are due to the underdamped character of the motion for this value of β . The transient time τ is approximately $6 \times 10^{-21} \text{ s}$, as can also be seen in Fig. 3. The analogous behavior of $\lambda_f(t)$ for dissipation that is 10 times as large is shown in Fig. 5.

As pointed out above, the quantity $\lambda_f(t)$ is the fission rate evaluated at the saddle point. However, for a realistic description it is necessary to evaluate the fission rate at the scission point. Because of the finite time needed by the system to traverse the distance from the saddle point to the scission point, it is necessary to modify $\lambda_f(t)$ as given by Eq. (3). We use the simple argument that the probability current that passes the saddle point at time t arrives at the scission point at time $t + \bar{t}$, where the mean saddle-to-scission time \bar{t} is determined below. We accordingly calculate the fission rate $\lambda_{sc}(t)$ at the scission point by putting

$$\begin{aligned} \lambda_{sc}(t) &= 0, \quad 0 \leq t \leq \bar{t}, \\ &= \lambda_f(t - \bar{t}), \quad t \geq \bar{t}, \end{aligned} \quad (4)$$

with $\lambda_f(t)$ given by Eq. (3). The approximate validity of this procedure has been demonstrated in Ref. 24.

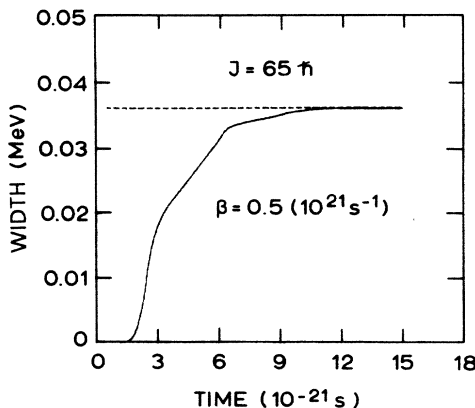


FIG. 4. Time dependence of the fission width $\hbar\lambda_f(t)$ at the saddle point for angular momentum $J = 65\hbar$ and reduced dissipation coefficient $\beta = 0.5 \times 10^{21} \text{ s}^{-1}$.

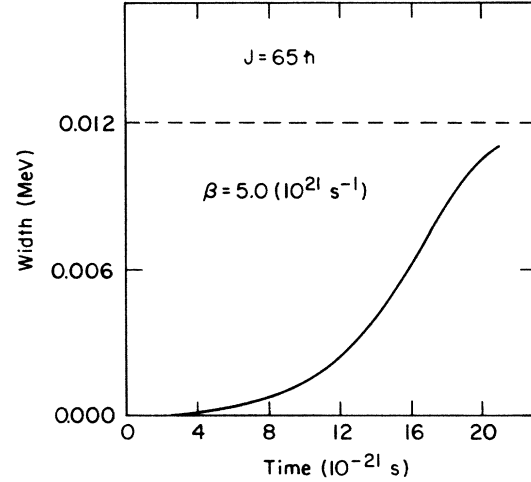


FIG. 5. Time dependence of the fission width $\hbar\lambda_f(t)$ at the saddle point for angular momentum $J = 65\hbar$ and reduced dissipation coefficient $\beta = 5.0 \times 10^{21} \text{ s}^{-1}$.

C. Mean saddle-to-scission time

The mean time \bar{t} needed for the system to traverse the distance from the saddle point to the scission point was calculated by use of the result^{7-9,24}

$$\bar{t} = \frac{2}{\omega_0} \left\{ \left[1 + \left[\beta / (2\omega_0) \right]^2 \right]^{1/2} + \beta / (2\omega_0) \right\} R \left[(\Delta V / T)^{1/2} \right],$$

where

$$R(z) = \int_0^z \exp(y^2) dy \int_y^\infty \exp(-x^2) dx$$

is a readily computed function studied and tabulated by Rosser²⁵ and ΔV is the difference in potential energy between the saddle and scission points. This analytical expression is derived from Kramers's stationary solution of the Fokker-Planck equation for an inverted oscillator. The dependence of the mean saddle-to-scission time \bar{t} upon the reduced dissipation coefficient β is shown in Fig. 6 for three values of angular momentum.

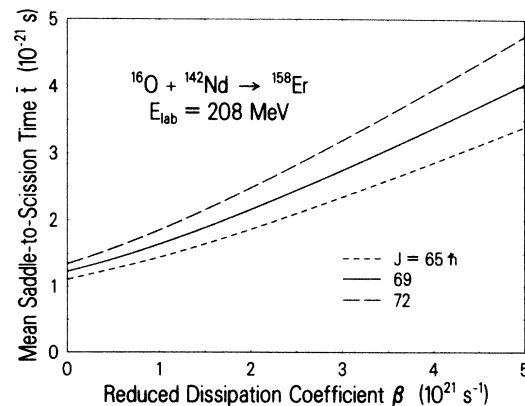


FIG. 6. Dependence of the mean saddle-to-scission time \bar{t} upon the reduced dissipation coefficient β , for three values of angular momentum J .

III. AVERAGE NEUTRON MULTIPLICITY PRIOR TO FISSION

In this section, we present the calculations of and the results for neutron multiplicities prior to the fission saddle point or scission, using the parametrizations (3) or (4), respectively, for the time dependence of the fission rate. We calculate the neutron multiplicities by following in time the competition between multiple particle emission and fission.

Let the index s , with $s=1,2,\dots$, label the nucleus reached after emission of $s-1$ neutrons prior to fission. In the case of ^{158}Er , this nucleus corresponds to $s=1$ and the nuclei reached by neutron decay are $^{159-s}\text{Er}$ for $s>1$. In the general case, the mass numbers A_s , values of angular momentum J_s , and average excitation energies E_s^* are given by

$$A_s = A_{s-1} - 1, \quad (5a)$$

$$J_s = J_{s-1} - \Delta J_s, \quad (5b)$$

and

$$E_s^* = E_{s-1}^* - B_{n,s-1} - 2T_{s-1} - \Delta E(s,s-1). \quad (5c)$$

In Eq. (5b), ΔJ_s is the angular momentum carried away by the neutron at the appropriate step. Phase-space arguments show that this is accompanied by a *reduction* of J_{s-1} . In Eq. (5c), $B_{n,s-1}$ is the neutron separation energy of the nucleus with mass number A_{s-1} , and T_{s-1} is the temperature of this nucleus. The energy difference $\Delta E(s,s-1)$ is due to the change of the energy of the yrast line (the rotating ground-state minimum) connected with the step $s-1 \rightarrow s$, corresponding to the change in angular momentum given by Eq. (5b). If not terminated previously by fission, the process of neutron emission terminates

at the latest when neutron emission becomes energetically impossible. We denote this step by s_0 , so that s_0-1 is the maximum number of pre-scission neutrons.

Let $P_s(t)$ be the occupation probability in time of the nucleus with mass number A_s . We describe the processes of neutron emission and fission by the set of coupled equations

$$\frac{d}{dt} P_s(t) = \Gamma'_{n,s-1} P_{s-1}(t) - [\Gamma_{n,s} + \hbar \lambda_s(t)] P_s(t). \quad (6)$$

Equations (6) have the general form of master equations, containing a gain term describing the feeding of P_s by the neutron decay of the previous nucleus, with associated probability $P_{s-1}(t)$, and a loss term accounting for both neutron decay and fission. The symbol $\lambda_s(t)$ stands for either the rate $\lambda_{f,s}(t)$ at the fission saddle point or the rate $\lambda_{sc,s}(t)$ at the scission point, as the case may be.

In evaluating the dependence of $\lambda_s(t)$ on A_s , we take into account the dependence of the temperature T on the excitation energy E_s^* , which is given by Eq. (5c). We also take into account the small dependences of the frequencies ω_0 and ω_1 on the index s . This is done by interpolating and extrapolating as functions of angular momentum J the values of ω_0 and ω_1 given in Table I. In Eqs. (6), the partial width $\Gamma'_{n,0} \equiv 0$ at the beginning of the chain and the width $\Gamma_{n,s_0} \equiv 0$ at the end of the chain. The difference between the neutron widths $\Gamma_{n,s}$ appearing in the loss terms that describe the decay of the nucleus A_s and the partial neutron widths $\Gamma'_{n,s}$ appearing in the gain term is described below. Equations (6) are solved numerically for the appropriate initial values of angular momentum, subject to the initial condition $P_s(0) = \delta_{s,1}$.

The neutron decay widths are calculated by use of the standard expression^{26,27}

$$\Gamma_n(E, J) = \frac{2}{2\pi\rho(E, J)} \sum_l \sum_{I=|J-l|}^{J+l} \int_0^{E-E_0(I)-B_n} d\epsilon T_l(\epsilon) \rho_n[E-E_0(I)-B_n-\epsilon, I]. \quad (7)$$

Here E is the total excitation energy including the energy of the yrast level, $E_0(I)$ is the energy of the yrast level of total angular momentum I , and T_l is the neutron transmission coefficient for a neutron with angular momentum l . The level density ρ_n of the residual nucleus following neutron emission is given by^{26,27}

$$\rho_n(E^*, J) = \frac{2J+1}{\sigma^3} (E^*)^{-5/4} \exp[2(a_n E^*)^{1/2}], \quad (8)$$

with σ denoting the spin-cutoff parameter. The level density ρ of the decaying nucleus is calculated in an analogous fashion. The transmission coefficients T_l are calculated both by use of the optical-model program of Ref. 26 and that contained in the statistical-model GROGI 2 program.²⁸ We find that both calculations yield identical results to within the required accuracy.

The partial neutron widths $\Gamma'_{n,s}$ appearing in the gain term of Eq. (6) differ from the widths $\Gamma_{n,s}$ defined by Eq. (7) because in the gain term only those neutron decays contribute after which fission is still competitive with

neutron decay. In calculating the partial widths $\Gamma'_{n,s}$, we therefore use Eq. (7) in a modified form. In the sum over I we take into account only terms for which $I \geq I_{\min}$, where I_{\min} is defined by the condition that the fission-barrier height and neutron separation energy are equal, namely $E_f(A, I_{\min}) = B_n$.

Equations (6) were solved numerically from time $t=0$ until time $t=t_{\max}$, where t_{\max} is twice the largest transient time τ deduced from the parametrization of all rates $\lambda_s(t)$ entering into these equations. For $t > t_{\max}$, all the rates $\lambda_s(t)$ were replaced by their asymptotic values Γ_f . Equations (6) can then be solved analytically, with the solutions expressed in terms of the new initial conditions $P_s(t_{\max})$, which are given numerically. In this way, the solutions $P_s(t)$ were obtained for all time $t \geq 0$.

The definitions of $P_s(t)$ and $\lambda_s(t)$ imply that the probability of emitting $s-1$ neutrons prior to fission is given by

$$p_s(J) = \int_0^\infty dt \lambda_s(t) P_s(t), \quad (9)$$

where J denotes the initial value of angular momentum for which the calculation was done. The average neutron multiplicity prior to fission therefore has the value

$$\nu(J) = \sum_{s=1}^{s_0} (s-1)p_s(J) / \sum_{s=1}^{s_0} p_s(J). \quad (10)$$

Equation (10) is evaluated for angular momenta in the range $65\hbar \lesssim J \lesssim 76\hbar$. The average neutron multiplicity $\langle \nu \rangle$ to be compared with the experimental data is then obtained from the expression

$$\langle \nu \rangle = \sum_J \nu(J) \sigma_{\text{abs}}(J) / \sum_J \sigma_{\text{abs}}(J). \quad (11)$$

For the absorption cross section $\sigma_{\text{abs}}(J)$ we use a rounded triangular distribution, although it turns out that $\langle \nu \rangle$ is quite insensitive to the precise form used.

Figure 7 shows the solutions $P_s(t)$ of Eqs. (6), for $\beta = 0.5 \times 10^{21} \text{ s}^{-1}$ and $J = 65\hbar$. The dashed curves are obtained by replacing the rates $\lambda_s(t)$ appearing in Eqs. (6) by the Bohr-Wheeler values Γ_f^0/\hbar , whereas the solid curves correspond to the choice $\lambda_s(t) = \lambda_{f,s}(t)$. We see clearly the enhancements of $P_s(t)$ in the full curves relative to the dashed curves, which lead to an increase in the neutron multiplicity.

The requirement that we must simultaneously reproduce the fission probability at low excitation energies imposes a relationship between a_f/a_n and β , where a_f and a_n are the level-density parameters for fission and neutron emission, respectively. In the quasistationary limit, this relationship can be obtained approximately from the constancy of Eq. (1) for the fission width. When the pre-exponential factors are neglected, the quantity Γ_f^0 that appears in Eq. (1) is proportional to $\exp\{2[a_f(E^* - E_f)]^{1/2}\}$. With $a_f/a_n = 1$ for $\beta = 0$, it then follows that

$$\frac{a_f}{a_n} = \left[1 + \frac{\ln \left\{ \left[1 + \left(\frac{\beta}{2\omega_0} \right)^2 \right]^{1/2} + \frac{\beta}{2\omega_0} \right\}}{2[a_n(E^* - E_f)]^{1/2}} \right]^2.$$

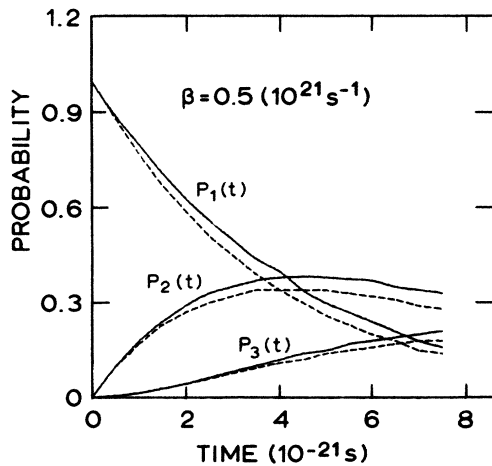


FIG. 7. Time dependence of the solutions $P_s(t)$ of Eqs. (6), for angular momentum $J = 65\hbar$ and reduced dissipation coefficient $\beta = 0.5 \times 10^{21} \text{ s}^{-1}$. The transient time τ is included in the solid curves, whereas the dashed curves refer to the Bohr-Wheeler value for the fission width.

Alternatively, for a given value of β the ratio a_f/a_n can be adjusted to reproduce the low-energy fission probability over a range of excitation energy E^* , which is the procedure followed here. Our result is shown by the dashed curve in Fig. 8.

The above quasistationary approximation is excellent for intermediate values of dissipation, where the transient time τ is relatively small. However, the long transient times that occur for both small and large dissipation noticeably affect the low-energy fission probability, and hence the dependence of a_f/a_n on β that is required to reproduce it. As shown by the solid curve in Fig. 8, when transients are included in the calculation of the low-energy fission probability,⁴ the values of a_f/a_n for both small and large dissipation are increased somewhat relative to those calculated in the quasistationary approximation. We use these results with transients included in the self-consistent calculations that follow.

Figure 9 shows the dependence of the average neutron multiplicity $\langle \nu \rangle$ on the reduced dissipation coefficient β for three cases. The short-dashed line marked SM at $\langle \nu \rangle = 1.6$ refers to the statistical model (SM) and corresponds to the predictions of the dissipation-independent Bohr-Wheeler formula, with $a_f/a_n = 1.0$. The long-dashed curve labeled T refers to transients and is obtained by putting $\lambda_s(t) = \lambda_{f,s}(t)$ in Eqs. (6); it does not include the influence of the mean saddle-to-scission time. As β increases, this curve initially decreases to a minimum value, then rises to a plateau, and finally decreases slowly. This results from the dependence of the transient time on β shown in Fig. 3 and the dependence of a_f/a_n on β shown in Fig. 8. The solid curve labeled SST refers to saddle-to-scission time and is obtained by putting

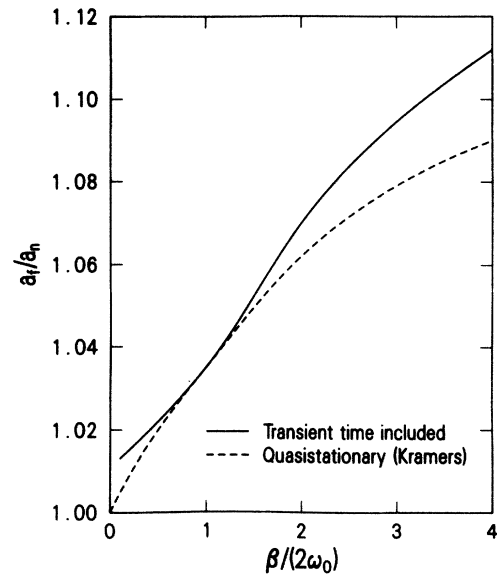


FIG. 8. Dependence of the ratio a_f/a_n of level-density parameters for fission and neutron emission upon the ratio $\beta/(2\omega_0)$ of the reduced dissipation coefficient to twice the barrier frequency, determined from the low-energy fission probability. The dashed curve gives the result when Eq. (1) alone is taken into account, and the solid curve gives the result when the transient time is also included.

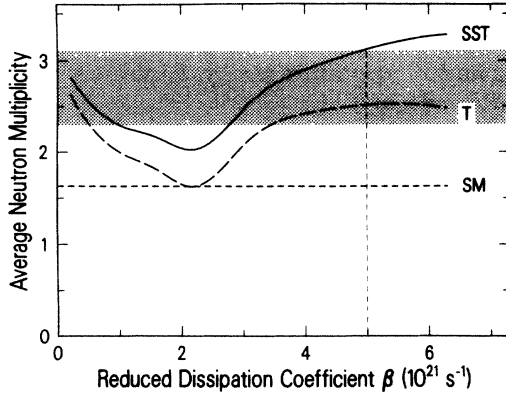


FIG. 9. Average neutron multiplicity $\langle \nu \rangle$ vs the reduced dissipation coefficient β . The curves labeled SM, T, and SST refer to the statistical model, the inclusion of transients, and the inclusion of both transients and the mean saddle-to-scission time, respectively. The experimental result (Ref. 14) is given by the shaded band, whose upper intersection with the solid curve determines the upper limit of β indicated by the vertical dashed line.

$\lambda_s(t) = \lambda_{sc,s}(t)$ in Eqs. (6). It includes both the transient time τ needed to build up the full current over the saddle point and the mean saddle-to-scission time $\bar{\tau}$ displayed in Fig. 6. The solid curve lies above the long-dashed curve by an amount that increases monotonically with increasing dissipation, but it is qualitatively similar and still contains a minimum.

For the reaction $^{16}\text{O} + ^{142}\text{Nd} \rightarrow ^{158}\text{Er}$ at 207 MeV that we have been considering, Gavron *et al.*¹⁴ find that the average number of neutrons emitted prior to fission is 2.7 ± 0.4 . This result is shown by the shaded band in Fig. 9. The inclusion of transients and the mean saddle-to-scission time therefore provides an interpretation of the enhanced neutron emission prior to fission. Also, by comparing the upper limit of our experimental result with the solid curve in Fig. 9, we obtain the limit $\beta \lesssim 5 \times 10^{21} \text{ s}^{-1}$ for the reduced nuclear dissipation coefficient. Although

the solid curve lies somewhat below the experimental band for intermediate values of dissipation, we do not feel that the comparison suggests two separate regions of allowed dissipation because of the sensitivity of the results to the input value of the fusion cross section and other details of the calculations.

IV. CONCLUSION

We have presented a formalism for taking into account the effects of transients and the mean saddle-to-scission time on neutron emission prior to fission. In terms of this formalism, we have provided an interpretation of the enhanced neutron emission prior to fission that is observed in the reaction $^{16}\text{O} + ^{142}\text{Nd} \rightarrow ^{158}\text{Er}$ at 207 MeV. This analysis has also determined the limit $\beta \lesssim 5 \times 10^{21} \text{ s}^{-1}$ for the reduced nuclear dissipation coefficient.

The particular reaction that we have analyzed was chosen because its high excitation energy leads to a high enhancement in the number of neutrons emitted prior to fission, which permits the determination of a useful upper limit of nuclear dissipation. Similar enhancements have also been observed experimentally in several other nuclear reactions. In future work, these reactions should be systematically analyzed by use of either the formalism presented here or—better still—by solving a multidimensional Fokker-Planck equation for the time evolution of the distribution function, starting from an initial configuration of two touching spheres. Such a study should not only set more stringent limits on nuclear dissipation, but also provide more accurate values of a_f/a_n than have been available in the past.

ACKNOWLEDGMENTS

We are grateful to H. C. Britt and F. Plasil for stimulating discussions. This work was supported by the Alexander von Humboldt Foundation, to which J. R. Nix is indebted for a follow up invitation under the Senior U. S. Scientist Award program, and the U. S. Department of Energy.

¹H. A. Kramers, *Physica* (The Hague) **7**, 284 (1940).

²N. Bohr and J. A. Wheeler, *Phys. Rev.* **56**, 426 (1939).

³P. Grangé and H. A. Weidenmüller, *Phys. Lett.* **96B**, 26 (1980).

⁴P. Grangé, J. Q. Li, and H. A. Weidenmüller, *Phys. Rev. C* **27**, 2063 (1983).

⁵H. A. Weidenmüller and J. S. Zhang, *Phys. Rev. C* **29**, 879 (1984).

⁶S. Hassani and P. Grangé, *Phys. Lett.* **137B**, 281 (1984).

⁷H. Hofmann and J. R. Nix, *Phys. Lett.* **122B**, 117 (1983).

⁸J. R. Nix, A. J. Sierk, H. Hofmann, F. Scheuter, and D. Vautherin, *Nucl. Phys.* **A424**, 239 (1984).

⁹J. R. Nix and A. J. Sierk, *Nucl. Phys.* **A428**, 161c (1984).

¹⁰A. Gavron, J. R. Beene, B. Cheynis, R. L. Ferguson, F. E. Obenshain, F. Plasil, G. R. Young, G. A. Petitt, M. Jääskeläinen, D. G. Sarantites, and C. F. Maguire, *Phys. Rev. Lett.* **47**, 1255 (1981); **48**, 835(E) (1982).

¹¹E. Holub, D. Hilscher, G. Ingold, U. Jahnke, H. Orf, and H.

Rosner, *Phys. Rev. C* **28**, 252 (1983).

¹²D. Ward, R. J. Charity, D. J. Hinde, J. R. Leigh, and J. O. Newton, *Nucl. Phys.* **A403**, 189 (1983).

¹³D. J. Hinde, R. J. Charity, G. S. Foote, J. R. Leigh, J. O. Newton, S. Ogaza, and A. Chatterjee, *Phys. Rev. Lett.* **52**, 986 (1984).

¹⁴A. Gavron, A. Gayer, J. Boissevain, H. C. Britt, J. R. Beene, B. Cheynis, D. Drain, R. L. Ferguson, F. E. Obenshain, F. Plasil, G. R. Young, G. A. Petitt, and C. Butler, *Phys. Rev. C* (to be published).

¹⁵X. Z. Wu, Y. Z. Zhuo, X. Z. Chang, Y. H. Yang, Z. Y. Ma, and F. R. Feng, *Commun. Theor. Phys. (Beijing)* **1**, 769 (1982).

¹⁶R. F. Feng, Y. Z. Zhuo, and J. Q. Li, *Chin. J. Nucl. Phys.* **6**, 113 (1984).

¹⁷F. Scheuter, C. Grégoire, H. Hofmann, and J. R. Nix, *Phys. Lett.* **149B**, 303 (1984).

- ¹⁸P. Möller and J. R. Nix, Nucl. Phys. **A361**, 117 (1981).
- ¹⁹S. Trentalange, S. E. Koonin, and A. J. Sierk, Phys. Rev. C **22**, 1159 (1980).
- ²⁰J. R. Nix and A. J. Sierk, Phys. Rev. C **15**, 2072 (1977).
- ²¹A. J. Sierk and J. R. Nix, Phys. Rev. C **21**, 982 (1980).
- ²²J. R. Nix, Nucl. Phys. **A130**, 241 (1969).
- ²³H. Delagrange, C. Grégoire, F. Scheuter, and Y. Abe, Grand Accélérateur National d'Ions Lourds Report No. GANIL-P-85-07, 1985 (unpublished).
- ²⁴K. H. Bhatt, P. Grangé, and B. Hiller, Phys. Rev. C **33**, 954 (1986).
- ²⁵J. B. Rosser, *Theory and Application of $\int_0^z \exp(-x^2)dx$ and $\int_0^z \exp(-p^2y^2)dy \int_0^y \exp(-x^2)dx$* (Mapleton House, New York, 1948), pp. 102–191.
- ²⁶A. Gavron, Phys. Rev. C **21**, 230 (1980).
- ²⁷S. E. Vigdor and H. J. Karwowski, Phys. Rev. C **26**, 1068 (1982).
- ²⁸J. R. Grover and J. Gilat, Phys. Rev. **157**, 802 (1967).

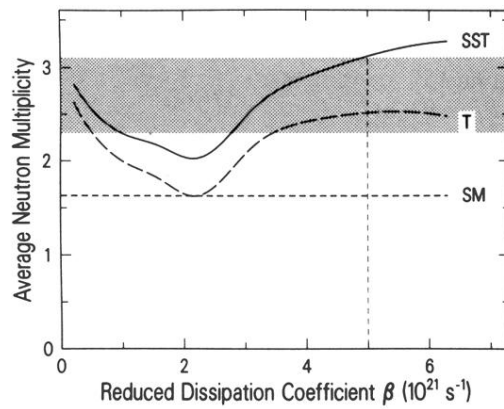


FIG. 9. Average neutron multiplicity $\langle \nu \rangle$ vs the reduced dissipation coefficient β . The curves labeled SM, T, and SST refer to the statistical model, the inclusion of transients, and the inclusion of both transients and the mean saddle-to-scission time, respectively. The experimental result (Ref. 14) is given by the shaded band, whose upper intersection with the solid curve determines the upper limit of β indicated by the vertical dashed line.